IEEE Access
Multidisciplinary | Rapid Review | Open Access Journal

Received 11 September 2022, accepted 17 October 2022, date of publication 26 October 2022, date of current version 9 November 2022.

Digital Object Identifier 10.1109/ACCESS.2022.3217233

RESEARCH ARTICLE

Modification of Pole Pitch and Pole Arc in Rotor Magnets for Cogging Torque Reduction in BLDC Motor

T. A. ANUJA[1], ARUN NOYAL DOSS M.[1], R. SENTHILKUMAR[1], RAJESH K. S.[2], (Member, IEEE), AND R. BRINDHA[1]

[1]Department of Electrical and Electronics Engineering, SRM Institute of Science and Technology, Kattankulathur 603203, India
[2]Department of Power Management, School of Business, University of Petroleum and Energy Studies, Dehradun 248007, India

Corresponding author: Arun Noyal Doss M. (arunnoyal@gmail.com)

ABSTRACT Cogging torque is an unfavorable hindrance in Permanent Magnet Brushless DC (PMBLDC) motor. In medium-low power PMBLDC motors, the surplus oscillations and intolerable noise happen because of the harmonic magnetic forces created by cogging torque. This paper introduces a new approach for the diminution of cogging torque. This method is based on placement irregularities in rotor magnets, and for this a new combination of pole arc and pole pitch was considered. The reference model has a pole pitch of 90° and pole arc of 63°. The new pole pitch is attained by the application of shifting technique on the permanent magnet and for the new pole arc it was resized. An analytical expression using the Virtual Work Method (VWM) Method was derived for locating the pole pitch and pole arc with nominal cogging torque in the PMBLDC motor. The technique is explored using 3D Finite Element Analysis (FEA). The comparison of the simulation and analytical results of cogging torque is accomplished. It is figured out that the cogging torque minimization in the analytical results exhibited acceptable agreement with FEA analysis.

INDEX TERMS BLDC motor, cogging torque, finite element analysis, virtual work method, pole pitch and pole arc.

I. INTRODUCTION

As the availability of permanent magnets increased, alloys of permanent magnets were used instead of electromagnets in the rotors of electric motors. The presence of permanent magnets helped motors to improve its performance like speed, torque etc. and at the same time reduced in size of the motor. The most commonly used permanent magnet motors are the Permanent Magnet Brushless DC motor (PMBLDC) and the Permanent Magnet Synchronous Motor (PMSM). Both the motors have its own advantages and disadvantages.

The BLDC motors are more effective compared to the conventional DC motors. Electronic commutator are used in BLDC motors instead of mechanical commutator of conventional DC motors. A closed loop control system is used to control the speed and position of the rotor. The hall sensors present in the stator detects the position of rotor and send signals to the controller in the VSI. The controller enables the particular transistors and send supply to the corresponding stator winding. The permanent magnet on the rotor is attracted by the energized stator winding and the very next moment another set of winding will be energized and the rotation of the rotor continuous in this way.

There are different types of BLDC motors are available, such as surface mounted permanent magnet, interior permanent magnet, spoke type BLDC motor, slotted BLDC motor, slot less BLDC motor and dual stator BLDC motor. Compared with conventional motors very high speed, compact in size, greater power density, and longer life span are some advantageousness of BLDC motor and it also have some disadvantages like vibrations, acoustic noise, reduction in flux density. Among these disadvantages the main obstruction for the smooth running of BLDC motor is cogging torque.

BLDC motor have permanent magnet on its rotor, and silicon steel laminations on its stator. There is always an

The associate editor coordinating the review of this manuscript and approving it for publication was Young Jin Chun.

attraction between the permanent magnets and silicon steel, as a result magnet interlocking happens between the rotor and stator. It restricts the smooth running of BLDC motor and produce vibration and noise. An extra energy is required to overcome this magnet locking and this is known as cogging torque. Vibration leads to the reduction in the life span of the motor and cogging torque causes to tone down the performance of the motor. On account of this, it is necessary to minimize the cogging torque in BLDC motor.

There are lot of techniques are available for minimizing the cogging torque. Some methods are based on the design, and some others are based on the soft computing techniques. The method of reducing the cogging torque in the design condition itself is more common than the second method. Skewing the permanent magnet, change the pole arc, pole pitch, and magnet thickness, irregularities in the placement of magnets are some methods based on the rotor. Just like that while considering the stator design, skewing the stator slot, providing bifurcations in the tooth are some commonly used methods.

Hwang et al. [1] proposed larger slot opening for minimizing the cogging torque and for this they recommended changes in the stator tooth width. Bretón et al. [2] suggested two different methods for the minimization of cogging torque in BLDC Motor. The first method is based on the asymmetrical magnetic distribution. To achieve this asymmetrical structure, the angle between the permanent magnet is kept different. In the second method they suggested auxiliary slots without any copper winding.

Bianchi and Bolognani [3] explained in detail the different methods for the reduction of cogging torque. Skewing the permanent magnet, changing the PM Pole arc width, PM Pole arc with different widths, are some effective methods for the rotor side and for stator side they recommended notches in the teeth. Caricchi et al. [4] tried a new design to compare various technical solutions. Such as PVC or Somaloy used in slot wedges, magnet skewing, angular shifting between the rotor discs, and mounting of magnets having distinct widths and arranged with either regularly spaced or in shortened pitch fashion on the discs are some methods.

Yoon [5] suggested that an effective slot angle with 18° is better for cogging torque reduction. Yang et al. [6] proposed an optimization method of improved domain elimination algorithm for minimizing the cogging torque of a permanent magnet motor. After this optimization an improved DEA and FEM are used to find the best pole arc coefficient. They concluded that the cogging torque is greatly reduced, and the computing time decreases notably by using the proposed technique.

González et al. [7] consider the effect of magnet shape and stator displacement on cogging torque reduction. They proposed skewing the magnet on the rotor side and displacement between stator sides. Hwang et al. [8] recommended a novel rotor pole shape that consists of a uniform surface and an eccentric surface. Shin et al. [9] recommended Latin hypercube sampling strategy to optimize a magnet pole shape. The proposed LHS algorithm consists of the multi-objective Pareto optimization and evolution strategy.

Lin et al. [10] suggested that the cogging torque is derived from the co-energy, not only in the air-gap, but also in the slot regions of the machine. The total cogging torque is synthesized from the contribution of each slot. The authors in reference [11] recommend stator side modification for reducing the cogging torque. They propose a T-shaped bifurcation in the stator tooth. Choi et al. [12] suggested that length to width ratio is an important parameter that affects the cogging torque. They recommended that stator core with skew angle is an effective method. This skew angle varied concerning the length to width ratio. Fazil and Rajagopal [13] proposed an airgap profile for minimizing the cogging torque in BLDC motor. The air gap profile is defined by dip, dip angle, leading edge, trailing edge, and inter magnet space. Aydin and Gulec [14] proposed a cost-effective magnet skewing for reducing the cogging torque. They recommended triangular skew shape for minimum cogging torque.

Rahman et al. [15] proposed an additional pushing assistant magnet and sub assistant magnet in the shape of spoke for reducing the cogging torque. By using the technique, the minimum cogging torque obtained is 0.7 Nm. U clamped magnetic poles, the authors in reference [16] tried to reduce the cogging torque. The authors in reference [17] suggested bifurcations in the stator for reducing the cogging torque in BLDC Motor. Park et al. [18] suggested a stator shape optimization technique. They provide notches in different angle and different sizes in stator for minimizing the cogging torque. The cogging torque of the optimized model was reduced more than 35.6%. Lee et al. [19] focused on stator skew model, they tried to increase the teeth thickness. The authors in reference [20] recommended bifurcations in the active region and a fuzzy logic controller for BLDC Motor. Hwang et al. [21] proposed a V-shaped magnet configuration for minimizing the cogging torque. The notches on the outer part of the magnet helps to reduce cogging torque. The authors [22] recommended that pole pitch shifting is a better method for minimizing the cogging torque. They suggested that 3° phase shift of rotor poles helps to minimize the cogging torque. García-Gracia et al. [23] proposed closing the slots by sliding in a pre-slot part made of the same ferromagnetic material as the stator.

The authors [24] suggested that for minimizing the cogging torque, rotor with asymmetrical structure is a better choice and to achieve this, they recommended rotor pole magnets with different thickness. Leitner et al. [25] recommended auxiliary slots and stator claw skewing for minimizing the cogging torque. They obtained 75% reduction in the cogging torque. Goryca et al. [26] suggested that a motor with the symmetric stator and asymmetric rotor or asymmetric stator and symmetric rotor is the best option for minimum cogging torque.

Han et al. [27] proposed shape optimization for minimizing the cogging torque. For this the RNM combined with GA and suggested rounded core shape of the outer rotor type is the

better choice. Markovic et al. [28] suggested that the best way to reduce the cogging torque is to use commercial software packages for the optimization in combination with the presented conformal mapping method. Lee et al. [29] proposed new stator and rotor designs for minimizing the cogging torque. They introduced partly enlarged air-gap made by rotor unequal out diameter and stator core structure with pole shoe modification. Kang et al. [30] derives mathematically the cogging torque and experimentally validated. Kim et al. [31] suggested that magnet shape and magnetization direction are the one of the important factor and optimization of magnet shape and magnetization direction helps to minimize the cogging torque.

A 4 -pole 12 -slot BLDC motor is considered for the entire research work. The basic structure designed has the pole arc is 63° and the pole pitch is 90°. In this technique of reducing the cogging torque a 1° phase shift is given to the permanent magnet in the rotor to change the pole pitch. After changing the pole pitch by 1°, the pole arc is changed from 63° to 67° in the same position. The cogging torque is measured at each change. Similarly, the pole pitch is changed from 1° to 7°. The cogging torque is measured in each pole pitch and pole arc combination and everything is compared at the end. An equation is derived based on the VWM and this technique is evaluated analytically. This is followed by a comparison of the analytical result and the simulation result.

The organization of the paper is: Proposed structure of BLDC Motor in section 2. The effect of changing pole arc and pole pitch on cogging torque is represented in section 3. Performance analysis is shown in section 4 and in section 5 comparative FEA analysis for cogging torque reduction techniques. The conclusion is shown in section 6.

II. PROPOSED STRUCTURE OF BLDC MOTOR

The stator construction of the BLDC motor is like a Permanent magnet Synchronous motor and an induction (asynchronous) motor. The rotor of the BLDC Motor has a Permanent Magnet, and the stator consists of winding is like the induction motor. BLDC Motor also contains Hall sensors and electronic servo systems. Hall sensors are placed in the stator to detect the rotor position and the servo system helps control the motor. Table 1 shows the design parameters and specifications of proposed BLDC Motor.

Figure 1 shows the extracted view of BLDC motor. The main dimensions depend on the specific electric loading and specific magnetic loading. A 4 -pole, 12- slots 1 hp Surface Mounted Permanent Magnet BLDC motor is the base model is used for summarizing the cogging torque. 48 V dc is used to give the excitation to the stator winding through the inverter. The rated current of the motor is 5.05 A, and the rated speed is 5000 rpm. The outer diameter of the motor is 60 mm, the stack height is 50 mm and the permanent magnet has 2.5 mm width. The outer and inner diameters of the rotor is 33 mm and 16. 7mm. The pole arc consider is 63°, pole pitch is 90° and the air gap length is 0.5m.

TABLE 1. Design parameters of motor.

Parameters	Specification
Power	1 hp
Supply Voltage	48 V
Rated Current	5.05 A
Number of poles	4
Number of Slots	12
Rated Speed	5000 rpm
Outer Diameter	60 mm
Stack Height	50 mm
Inner Diameter Rotor	16.7 mm
Outer Diameter Rotor	33 mm
Air gap Thickness	0.5 mm
Magnet Thickness	2.5 mm
Pole Arc	63°

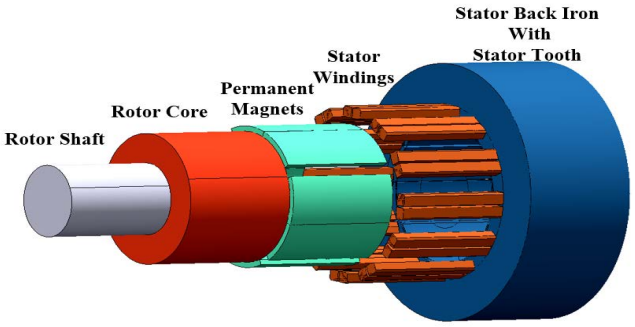

FIGURE 1. Extracted view of BLDC motor.

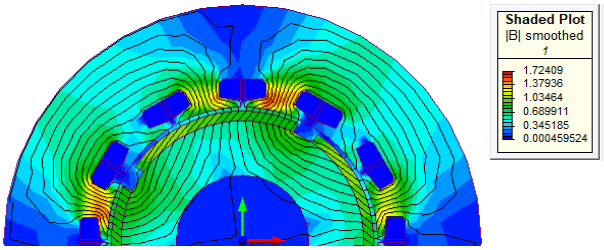

FIGURE 2. Flux density distribution in symmetrical structure.

FLUX PLOT ANALYSIS

Flux plot analysis is a common FEA analysis technique. This analysis aids in determining the usable, normal, and tangential flux densities in the air gap, which play the most important role in the BLDC motor's performance. The flux density is uniform throughout the BLDC motor. The FEA result is multicolored, with each hue representing the flux density fluctuations. Yellow shows the highest flux density distribution, whereas red denotes the hotspot. The motor is harmed as a result. It causes damage to the motor. Figure 2 shows the flux density distribution in symmetrical structure.

TABLE 2. FEA result of conventional BLDC motor.

Model	Normal flux Density (Wb/m^2)	Tangential Flux Density (Wb/m^2)	Cogging Torque (Nm)
Conventional BLDC Motor	0.71	0.95	0.54

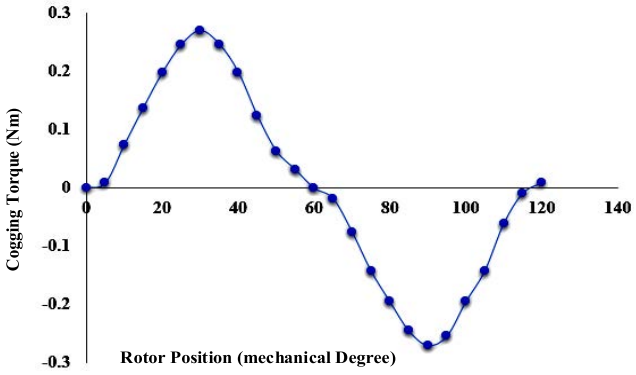

FIGURE 3. Cogging torque of conventional BLDC motor.

Table 2 shows the FEA result of conventional BLDC motor. Normal Flux density is 0.71 Wb/m^2, tangential flux density is 0.95 Wb/m^2 and cogging torque is 0.54 Nm Figure 3 shows the graphical representation of cogging torque in conventional BLDC Motor.

III. EFFECT OF CHANGING POLE ARC AND POLE PITCH ON COGGING TORQUE

A better way to reduce the cogging torque is to optimize the pole arc and pole pitch of the permanent magnet. To obtained the better combination of pole pitch and pole arc having minimum cogging torque, the first step is to give a 1° phase shift to the pole pitch and then changes the pole arc from 63° to till 67°. And tried out the method till the pole pitch phase shift equal to 7°. The cogging torque is measured in each pole pitch and pole arc combination and everything is compared at the end. An equation is derived based on the VWM and this technique is evaluated analytically. This is followed by a comparison of the analytical result and the simulation result. The procedure for finding combination of the pole arc and pole pitch with minimum cogging torque is shown in Figure 4.

A. ANALYTICAL EXPRESSION OF COGGING TORQUE

According to [34] cogging torque is produced as a result of interaction between the PMs and the slotted armature. Because of this interaction, in the absence of current also an energy variation is happened inside the motor.

$$E_v = E_{v.i} + E_{v\ airgap} + E_{v\ pm} \tag{1}$$

Here $E_{v.i}$, $E_{v\ airgap}$ and $E_{v\ pm}$ are the energy variation in the iron, air gap and permanent magnet. When compared with energy variation in air gap and PM, only a minor variation is occur in iron. Therefore

$$E_v \cong E_{v\ airgap} + E_{v\ pm} \tag{2}$$

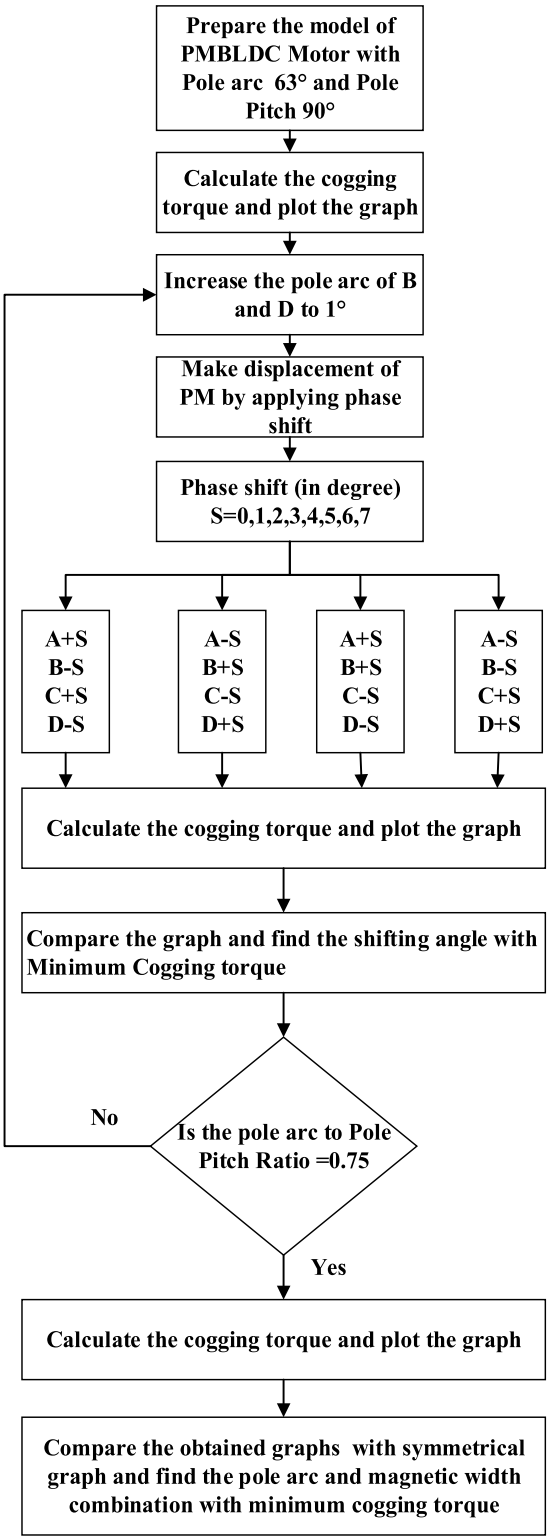

FIGURE 4. Flow chart for finding the pole Arc and pole pitch with minimum cogging torque.

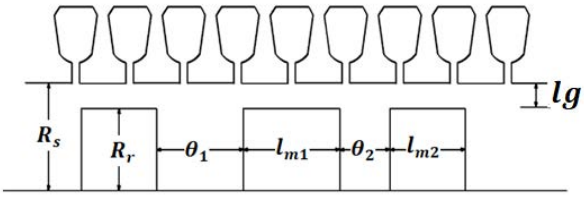

FIGURE 5. Simplified representation of stator and asymmetrical rotor PMs.

The cogging torque can be estimated using the energy approach by comparing the energy fluctuation with the angular velocity. The VWM is used for deriving the analytical expression. The cogging torque can be stated as

$$T_{cog} = -\frac{\partial E_v}{\partial \alpha} \tag{3}$$

Here, α is the angle between a certain tooth center and certain permanent magnet center. From equation 2 the energy in the motor includes the energy in the air gap and that in the permanent magnet. Then energy in the motor can be expressed as

$$E_v = -\frac{1}{2\mu_0} \iiint B^2 dv \tag{4}$$

The energy Ev depends on the structure data, performance of permanent magnet and the relative position α. At the relative position α, the expression of air gap flux density at the surface of armature can be expressed as

$$B(\theta, \alpha) = B_r(\theta) \frac{I_m}{l_m + g(\theta, \alpha)} \tag{5}$$

where, $B_r(\theta)$, $g(\theta, \alpha)$ and l_m are the remanence, effective length of the air gap length and length of permanent magnet.

Substituting equation (5) in (4), then

$$E_v = \frac{1}{2\mu_0} \iiint (B_r(\theta) \frac{l_m}{l_m + g(\theta, \alpha)})^2 dv \tag{6}$$

$$E_v = \frac{1}{2\mu_0} \iiint B_r^2(\theta). \left[\frac{l_m}{l_m + g(\theta, \alpha)}\right]^2 dv \tag{7}$$

The Fourier expansion of

$$B_r^2(\theta) = a_0 + \sum_{n=1}^{\infty} a_n \cos 2np\theta \tag{8}$$

where, p is the number of poles and θ is the pole pitch.

Figure 5 shows the simplified representation of stator and asymmetrical rotor. The rotor has asymmetrical magnets, with pole magnets of varying widths lm1 and lm2. To make the calculation easier, we compute the cogging torque of the machine with the pole arc lm1 first, then the cogging torque with the pole arc lm2. The effective magnetic energy of the machine with asymmetrical rotor magnets is then calculated by linearly superimposing these and calculating the average.

The analytical statement of cogging torque for asymmetrical magnet can be expressed as

$$T_{cog} = \frac{\pi z L_s}{4\mu_0} (R_r^2 - R_s^2) \sum_{n=1}^{\infty} B_{rsanz} \sin ns\alpha \tag{9}$$

TABLE 3. Analytical results of cogging torque with Different pole pitch and pole arc combination.

Shifting Angle	Pole Pitch A-B, B-C, C-D, and D-A	Pole Arc (°) A, B, C and D	Cogging Torque (Nm)
0°	90°,90°,90°,90°	63°,63°63°,63°	0.54
1°	91°,89°,91°,89°	63°,65°,63°,65°	0.31
2°	92°,88°,92°,88°	63°,65°,63°,65°	0.29
3°	87°,93°,87°,93°	63°,66°,63°,66°	0.16
4°	94°,86°,94°,86°	63°,65°,63°,65°	0.32
5°	85°,95°,85°,95°	63°,64°,63°,64°	0.30
6°	96°,84°,96°,84°	63°,65°,63°,65°	0.39
7°	97°,83°,97°,83°	63°,65°,63°,65°	0.34

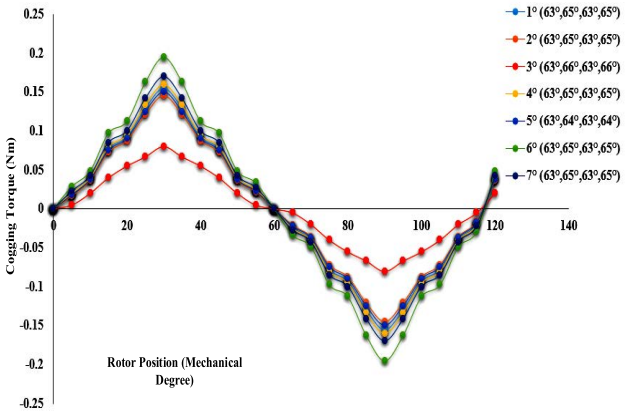

FIGURE 6. Graphical representation of cogging torque.

$$B_{rsanz} = \frac{2B_{rs}^2}{ns\pi} \sin \frac{ns\pi \alpha_p}{2p} \sum_{k=1}^{2p} \cos ns \left[\frac{\pi}{p}(k-1)\right] \tag{10}$$

where s is the slot number, Ls is the stator length,Rr is the outer radius of the rotor, Rs is the inner radius of the stator,

Table 3 shows the analytical results of cogging torque for every combination of pole pitch and pole arc. Figure 6 shows the graphical representation of cogging torque.

B. MANIPULATION OF COGGING TORQUE BY FEA

The goal of this project is to manipulate the pole pitch and pole arc combination with the least amount of cogging torque possible. Pole pitch is 90°, while pole arc is 63°. Shifting the permanent magnet from 1° to 7° changes the pole pitch. The pole arc is also altered from 63° to 67° for each pole pitch modification. Each combination's cogging torque is determined. This result is compared, and the combination that produces the least cogging torque is chosen. Figure7 shows the FEA result of the Basic structure having 90° pole pitch and 63° pole arc. The mechanical and electromagnetic characteristics and cogging torque are shown in figure.

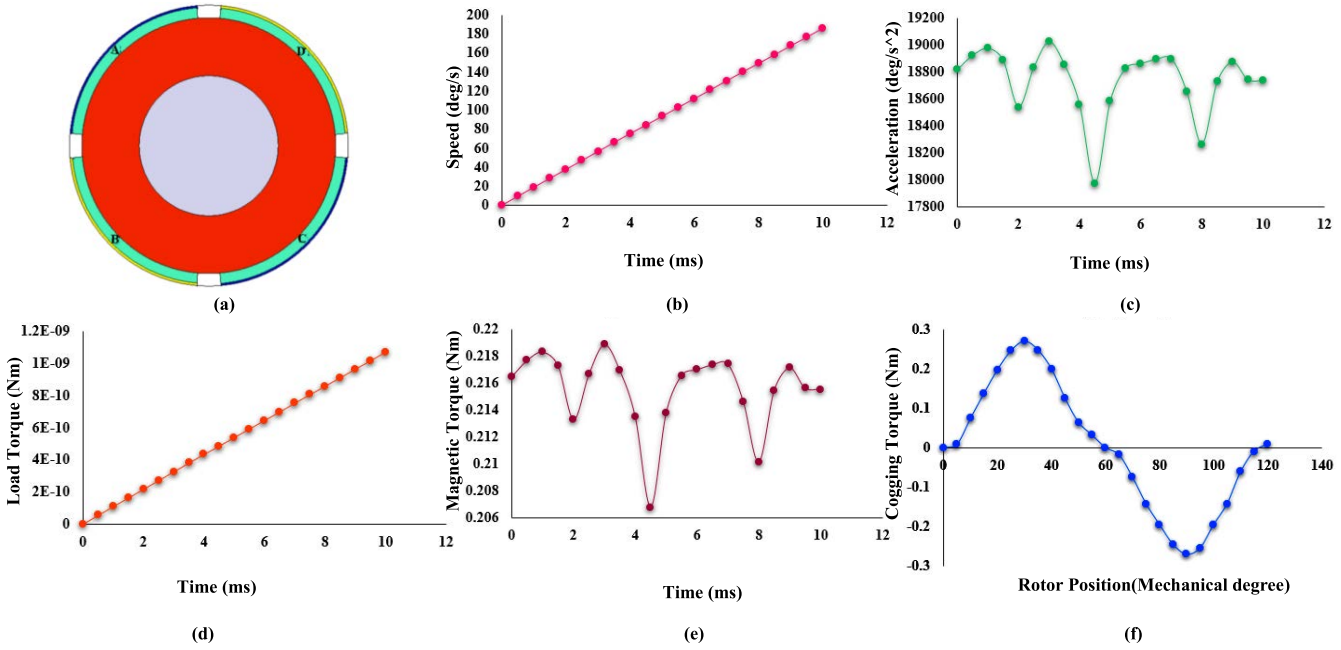

FIGURE 7. (a) The basic structure of Rotor, graphical representation of (b) speed (c) acceleration (d) Load Torque (e) Magnetic Torque (f) Cogging Torque.

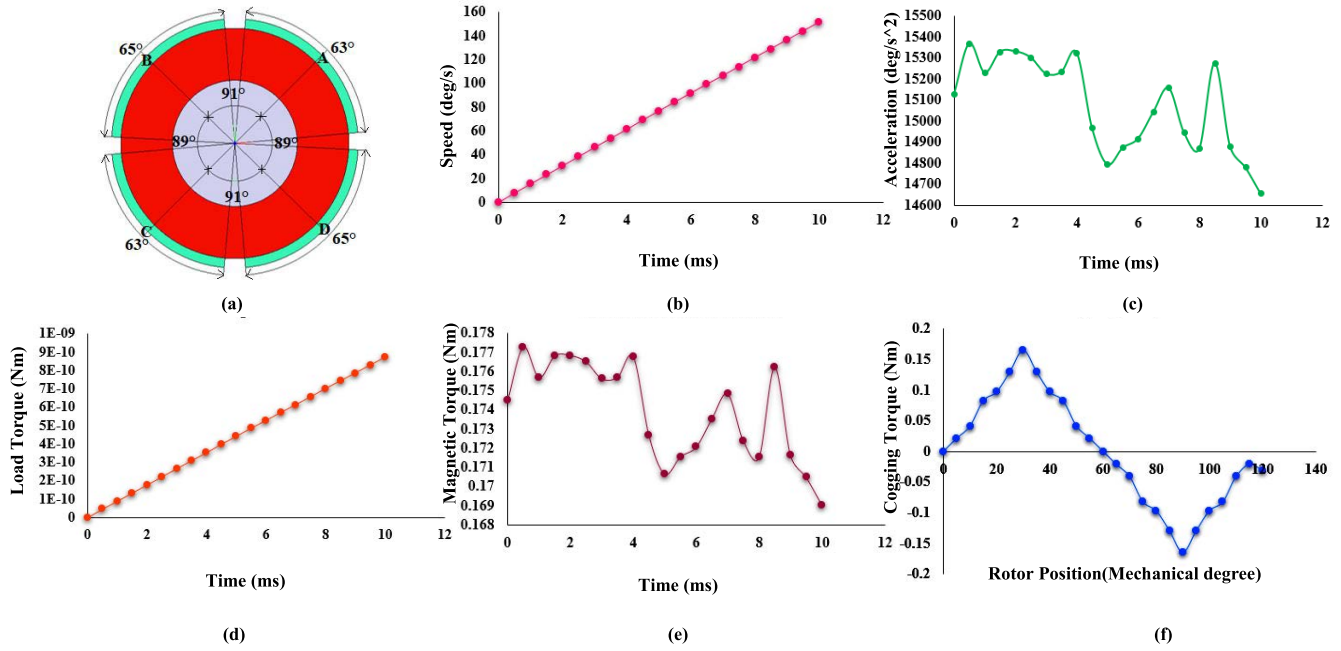

FIGURE 8. (a) Combination of pole arc with 1° phase shift, graphical representation of (b) speed (c) acceleration (d) Load Torque (e) Magnetic Torque (f) Cogging Torque.

In first step the 1° magnet shift is considered. As a result, the best combination of pole pitch will be (A-B (91°), B-C (89°), C-D (91°), and D-A (89°)). In this pole pitch combination, the pole arc changes from 63° to 67° is tried out. The resulting best combination of the pole arc will be (A-63°, B-65°, C-63°, D-65°). In this combination the cogging torque will be 0.33Nm. Figure 8 shows the better combination of pole pitch and pole arc of 1° phase shift. The mechanical and electromagnetics are also shown in the figure.

In the next step 2° magnet shift is considered. Here the best combination is obtained A-B (92°), B-C (88°), C-D (92°), and D-A (88°). Here the minimum cogging torque of 0.3Nm is obtained when the pole arc combination is (A-63°, B-65°, C-63°, D-65°). Figure 9 shows the better combination of pole pitch and pole arc of 2° phase shift. The mechanical and electromagnetics are also shown in the figure. When 3° magnet shift is applied, the combination of pole pitch is obtained A-B (87°), B-C (93°), C-D (87°), D-A (93°).

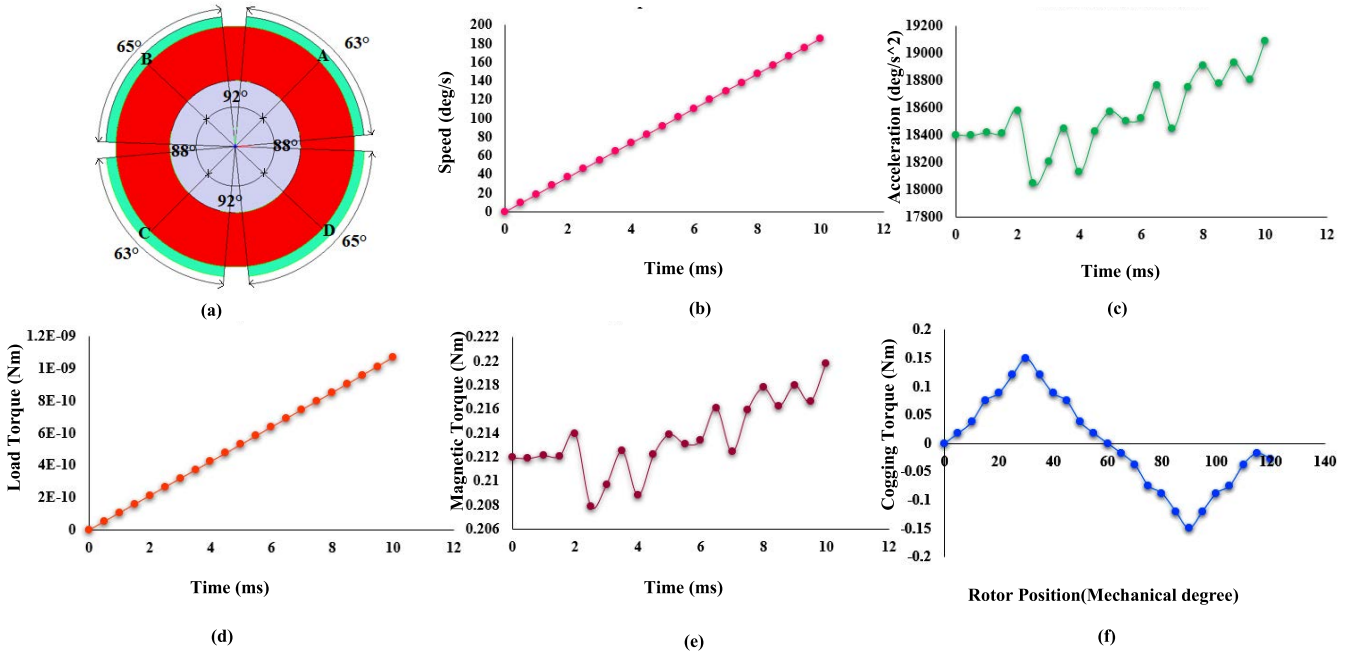

FIGURE 9. (a) Combination of pole arc with 2° phase shift, graphical representation of (b) speed (c) acceleration (d) Load Torque (e) Magnetic Torque (f) Cogging Torque.

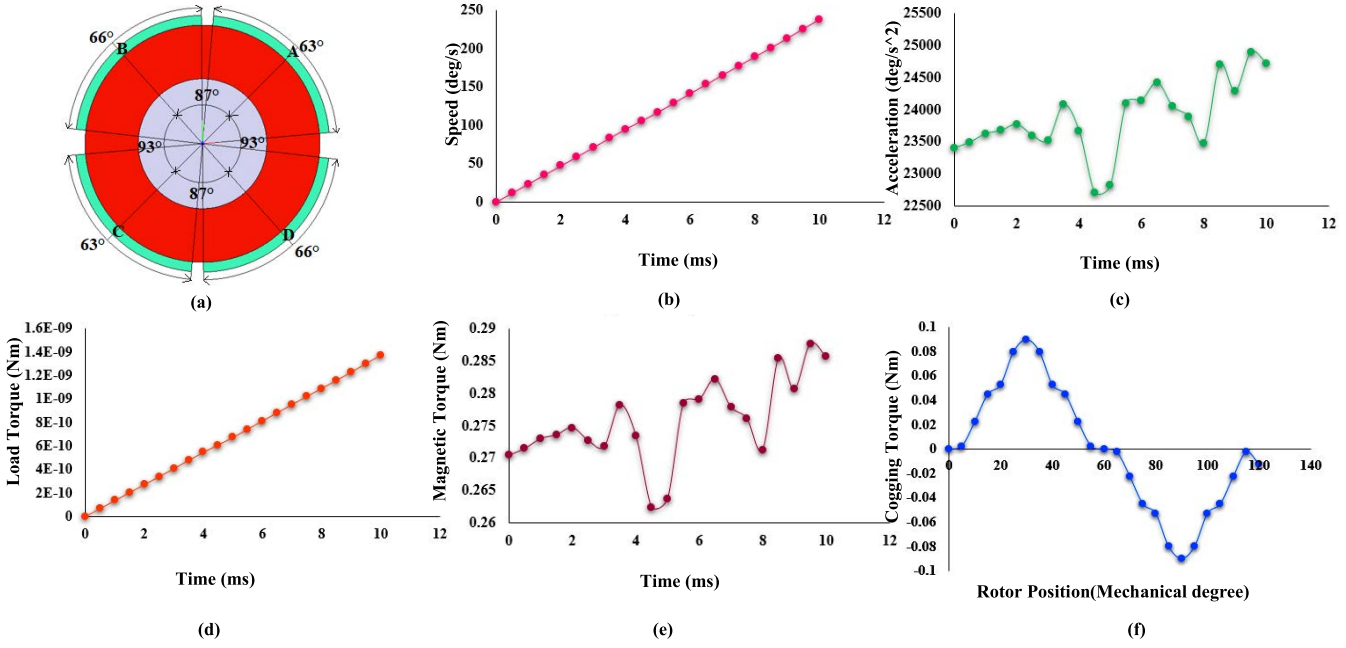

FIGURE 10. (a) Combination of pole arc with 3° phase shift, graphical representation of (b) speed (c) acceleration (d) Load Torque (e) Magnetic Torque (f) Cogging Torque.

Whereas the best combination of pole arc is (A-63°, B-66°, C-63°, D-66°) and the cogging torque value is 0.18Nm. Figure 10 shows the better combination of pole pitch and pole arc of 3° phase shift. The mechanical and electromagnetics are also shown in the figure.

After the 3° shifting the permanent magnets are shifted to 4°. Then the pole pitch value is obtained A-B (94°), B-C (86°), C-D (94°), and D-A (86 °). For this combination the minimum cogging torque obtained is 0.36 Nm. Which is obtained with the pole arc combination of rotor magnets is A-63°, B-65°, C-63°, D-65°. Figure 11 shows the better combination of pole pitch and pole arc of 4° phase shift. The mechanical and electromagnetics are also shown in the figure. In the next step 5° shift for permanent magnets is tried out. At this condition the pole pitch value is A-B (85°), B-C (95°), C-D (85°), and D-A (95°). Minimum cogging torque

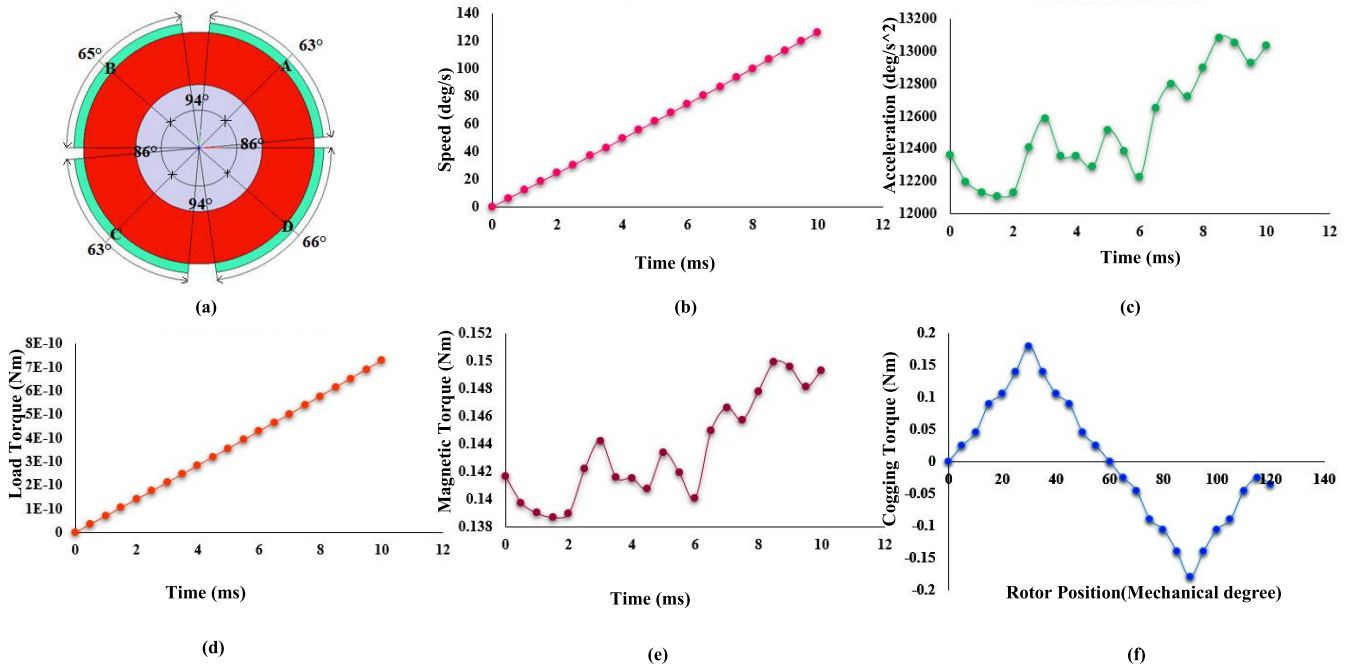

FIGURE 11. (a) Combination of pole arc with 4° phase shift, graphical representation of (b) speed (c) acceleration (d) Load Torque (e) Magnetic Torque (f) Cogging Torque.

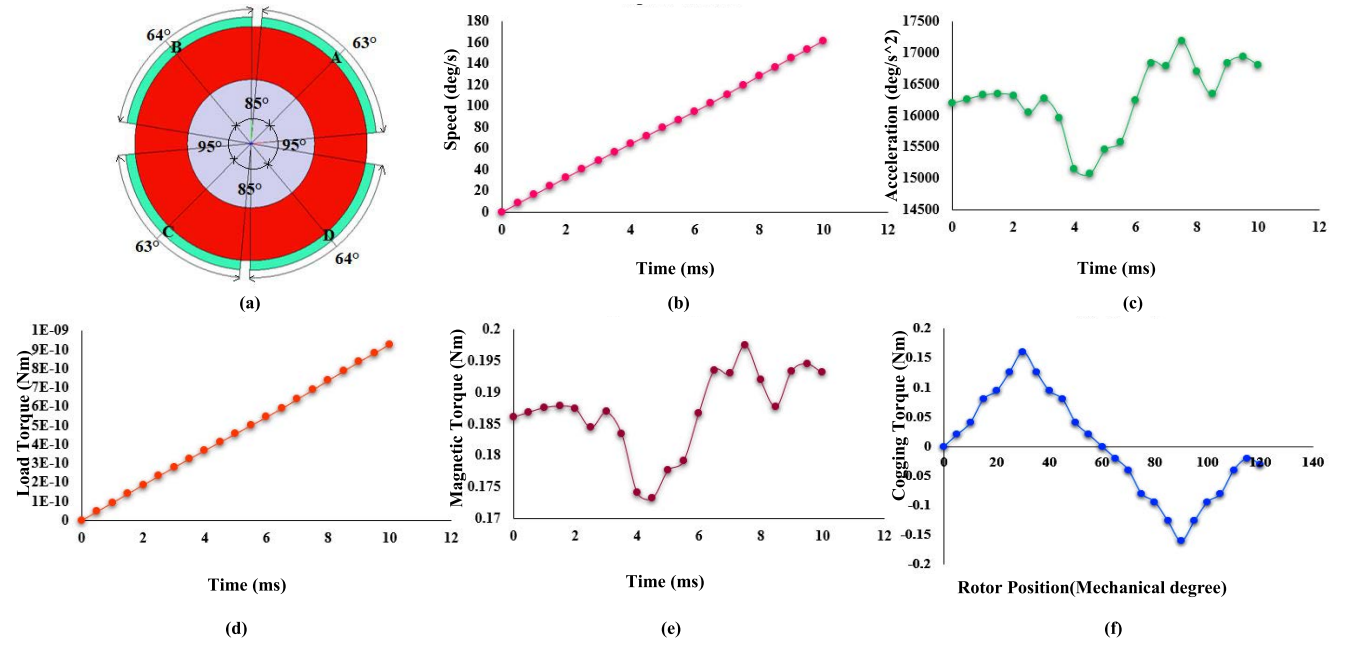

FIGURE 12. (a) Combination of pole arc with 5° phase shift, graphical representation of (b) speed (c) acceleration (d) Load Torque (e) Magnetic Torque (f) Cogging Torque.

of 0.32 Nm is obtained with the pole arc combination of rotor magnets is A-63°, B-64°, C-63°, D-64°. Figure 12 shows the better combination of pole pitch and pole arc of 5° phase shift. The mechanical and electromagnetics are also shown in the figure.

In the next step the shift to the permanent magnet is 6°. The pole pitch value obtained for this combination is A-B (96°), B-C (84°), C-D (96°), and D-A (84°). The better combination of reduced pole arc for this condition is A-63°, B-65°, C-63°, D-65° with minimum cogging torque is 0.41 Nm. Figure 13 shows the better combination of pole pitch and pole arc of 6° phase shift. The mechanical and electromagnetics are also shown in the figure.

7° magnet shift is applied to the permanent magnet and the pole pitch value is A-B (97°), B-C (83°), C-D (97°), and D-A (83°). Minimum cogging torque of 0.37 Nm is obtained

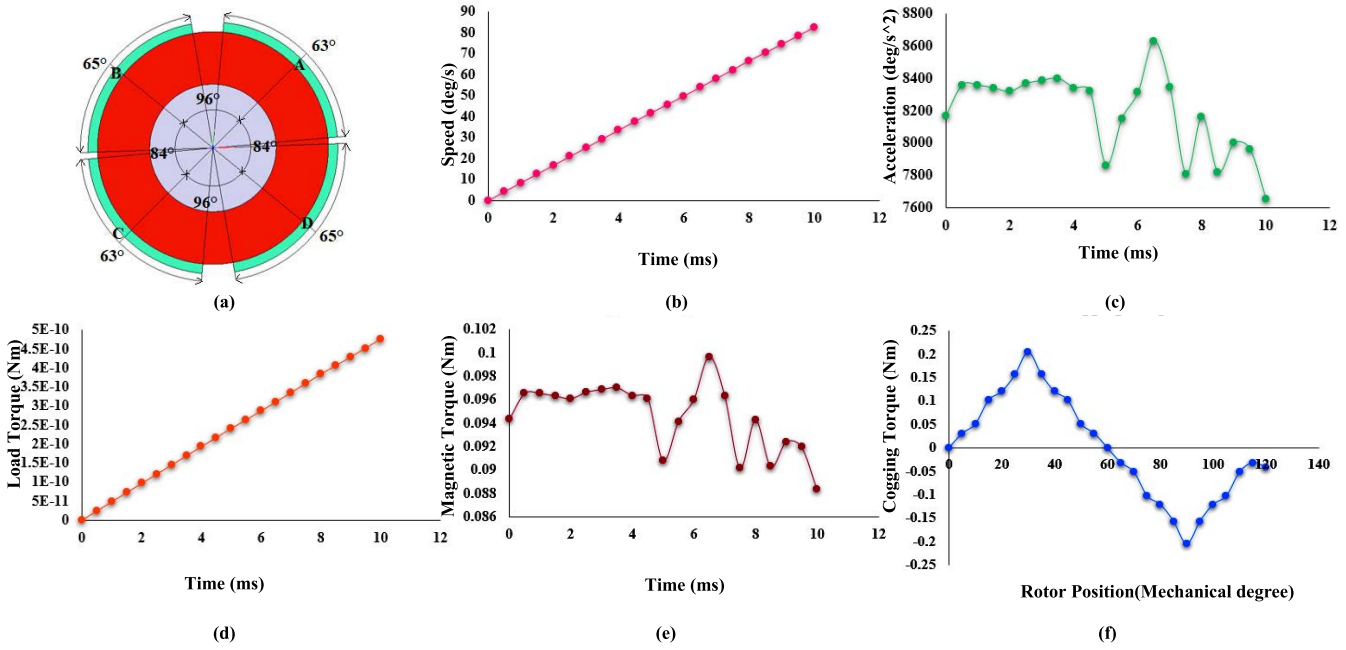

FIGURE 13. (a) Combination of pole arc with 6° phase shift, graphical representation of (b) speed (c) acceleration (d)Load Torque (e) Magnetic Torque (f) Cogging Torque.

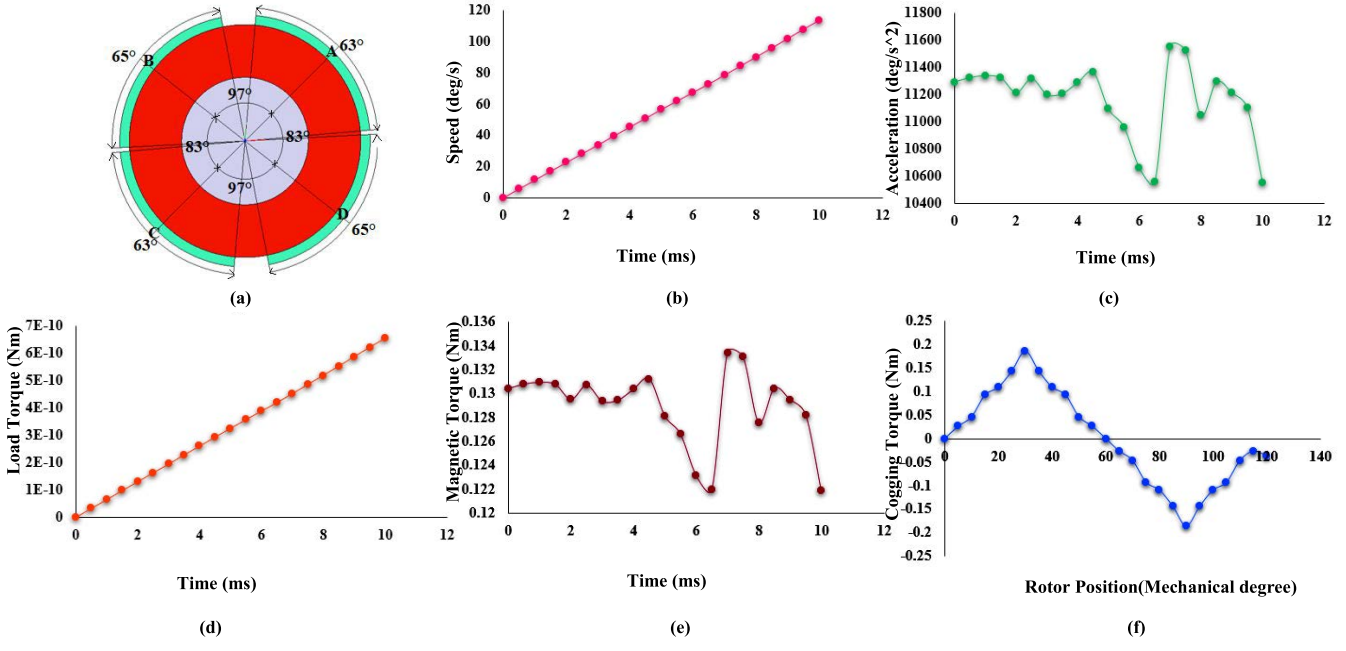

FIGURE 14. (a) Combination of pole arc with 7° phase shift, graphical representation of (b) speed (c) acceleration (d) Load Torque (e) Magnetic Torque (f) Cogging Torque.

with the combination of reduced pole arc is A-63°, B-65°, C-63°, D-65°. Figure 14 shows the better combination of pole pitch and pole arc of 7° phase shift. The mechanical and electromagnetics are also shown in the figure.

Electromagnetic torque refers to rotational motion caused by electromagnetic forces. It's the result of a time-varying electromagnetic field caused by a changing voltage or rotor motion with the stator as a reference. It is the torque required to begin the motor's revolution. It's usually the same as the load torque. The load torque is the output of electromagnetic torque (torque produced over an armature in an air gap). Parameters like damping torque and moment of inertia plays an effective role while considering the machine design, this may also have an effect on final torque value.

The torque induced by the load current over the shaft is known as load torque. Load torque depends upon the speed

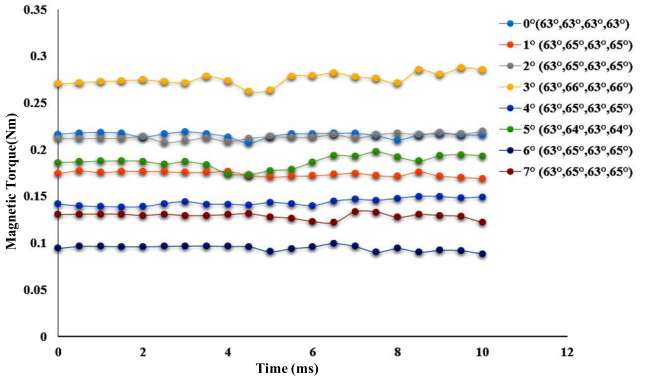

FIGURE 15. Comparison of Magnetic torque after applying different pole pitch and pole arc combination.

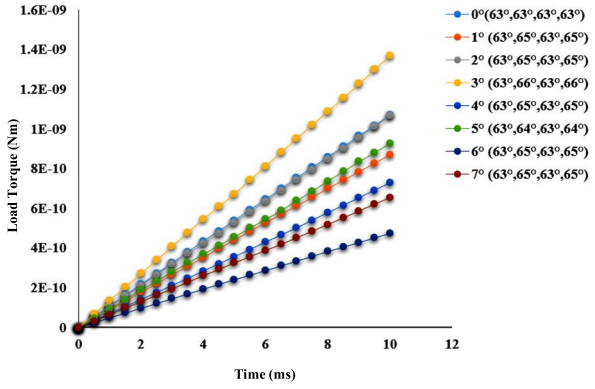

FIGURE 16. Comparison of Load torque after applying different pole pitch and pole arc combination.

which is a direct factor for varying the speed which also affects the electromagnetic torque..Because load torque is related to load, when load torque increases, the speed lowers and the electromagnetic torque falls as well. Figure 15 and 16 shows the comparison of magnetic torque and load torque of different pole pitch and Pole Arc combination. From the performance characteristics it is concluded that rotor with 3° pole pitch and the pole arc (63°, 66°, 63°, 66°) has obtained the maximum load torque.

Net torque is the sum of the individual torques. In no-load condition the net torque is almost equal to magnetic torque. Figure 17 shows the comparison of net torque while applying different pole pitch and Pole Arc combination. From the Figure it is well clear that when the pole pitch shift is 3° and the Pole Arc (63°, 66°, 63°, 66°) have the maximum net torque.

Figure 18 shows the comparison of speed of BLDC motor after applying different pole pitch and magnet shift combination and from the speed curve it is very clear that the starting itself the combination of pole pitch 3° and pole arc (63°, 66°, 63°, 66°) has attained more speed than other combination. Acceleration is also greater for this combination than other combination. The comparison of acceleration after applying different pole pitch and pole arc combination is shown in Figure 19.

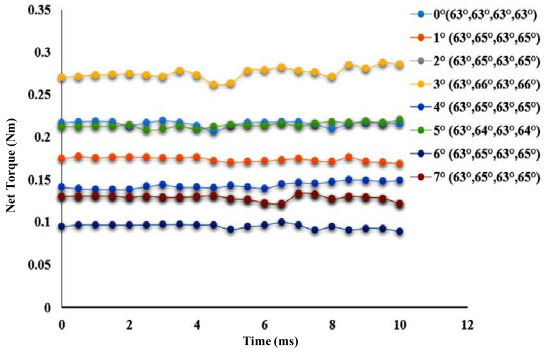

FIGURE 17. Comparison of Net torque after applying different pole pitch and pole arc combination.

TABLE 4. Comparison of best combination of pole pitch and pole arc with minimum cogging torque.

Pole Pitch A-B, B-C, C-D, and D-A		Pole Arc (°) A, B, C and D	Cogging Torque (Nm)
1°	91°,89°,91°,89°	63°,65°,63°,65°	0.33
2°	92°,88°,92°,88°	63°,65°,63°,65°	0.3
3°	87°,93°,87°,93°	63°,66°,63°,66°	0.18
4°	94°,86°,94°,86°	63°,65°,63°,65°	0.36
5°	85°,95°,85°,95°	63°,64°,63°,64°	0.32
6°	96°,84°,96°,84°	63°,65°,63°,65°	0.41
7°	97°,83°,97°,83°	63°,65°,63°,65°	0.37

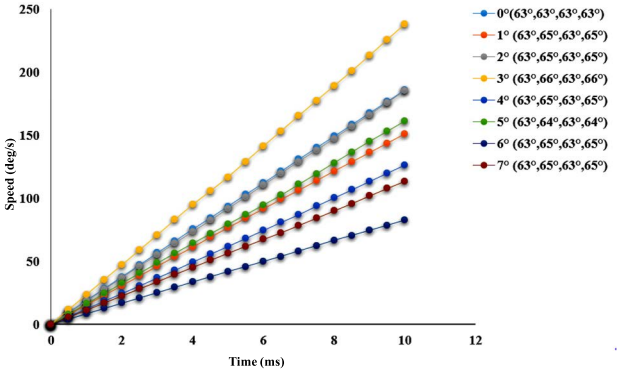

FIGURE 18. Comparison of speed after applying different pole pitch and pole arc combination.

When compared with the basic structure, the structure shown in figure 10 shows the supreme characteristics like speed, acceleration, load torque and magnetic torque.

Table 4 shows the FEA result of the BLDC motor after the application of cogging torque reduction technique. From the Table 6 when the pole pitch is 1° and pole arc is 63° (A&C) and 65° (B&D) the cogging torque is 0.33 Nm. When this pole pitch is increased to 2°, the cogging torque is reduced to 0.3 Nm. Then the pole arc is 63° (A&C) and 65° (B&D). In the next step the pole pitch is increased to 3° and the pole arc is 63°(A&C) and66°(B&D), the cogging torque is reduced to 0.18Nm. Again, the pole pitch is increased to 4°

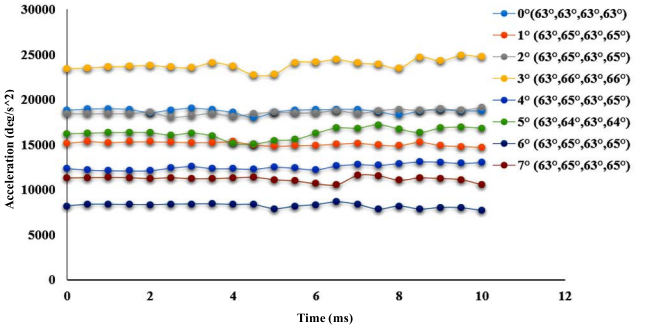

FIGURE 19. Comparison of acceleration after applying different pole pitch and pole arc combination.

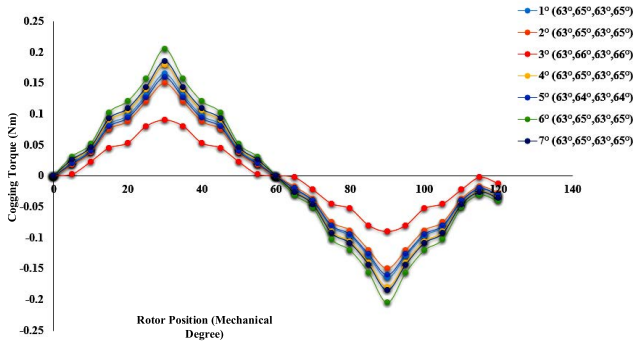

FIGURE 20. Comparison of cogging torque with different pole pitch and pole arc combination.

the cogging torque is 0.36 Nm, then the pole arc is 63° (A&C) and 65° (B&D). The cogging torque obtained is 0.32 Nm when the pole pitch is 5° and pole arc is 63° (A&C) and 64° (B&D). In the next step the cogging torque value is 0.41 Nm. Then the pole pitch value is 6° and the pole arc is 63° (A&C) and 65° (B&D). When the pole pitch is increased to 7° and the pole arc is 63° (A&C) and 65° (B&D), then the cogging torque is 0.37 nm. Figure 20 shows the comparison of cogging torque of different combination of pole pitch and pole arc.

From the above comparison when step the pole pitch is increased to 3° and the pole arc is 63° (A&C) and66° (B&D), obtained the lowest cogging torque 0.18Nm. Compare with the base rotor, the new asymmetrical structure has a 66.6% reduction in the cogging torque.

C. FLUX PLOT ANALYSIS

Flux plots analysis is a quick way to look at the flux density distribution and estimate how much useful flux is available. The flux plots of the conventional motor and the suggested BLDC motor are shown in Figure 21. The usable flux is shown in yellow on the flux charts. The usable flux density of the basic design is 1.37 Wb/m^2, while the proposed design is 1.41 Wb/m^2. When applying pole pitch and pole arc change in the rotor magnets, the flux density increases. It causes the reluctance to change comparatively better than the existing method and results in cogging torque reduction.

Table 5 compares the flux density of symmetrical and asymmetrical magnets in the BLDC Motor, The symmetrical

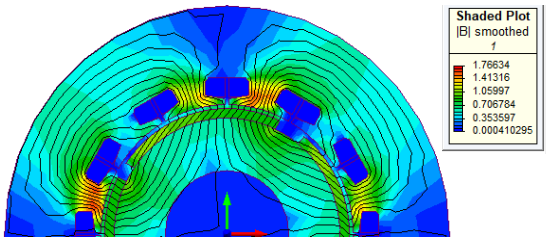

FIGURE 21. Flux plots in proposed BLDC motor.

TABLE 5. Flux density comparison of Symmetrical and asymmetrical Rotor PMs.

Model	Rotor with Symmetrical PMs.	Rotor with Asymmetrical PMs.
Normal Flux Density Wb/m^2	0.71	0.82
Tangential Flux Density Wb/m^2	0.95	1.1
Cogging torque (Nm)	0.54	0.18

rotor's normal flux density is 0.71 Nm, while the asymmetrical rotor's is 0.82 Nm. The tangential flux density of a symmetric rotor is 0.95 Wb/m^2, while that of an asymmetric rotor is 1.1 Wb/m^2. Compared with the conventional structure the normal flux and tangential flux densities of proposed structure is increased. The cogging torque for symmetrical structure is 0.54Nm and for asymmetrical rotor it is 0.18 Nm. While considering the BLDC motor with symmetric rotor magnets the motor with asymmetric rotor magnet obtained a 66.6% reduction in the cogging torque. The comparison of flux densities and cogging torque are shown in Figure 22.

IV. PERFORMANCE ANALYSIS

The important performance characteristics of BLDC motor are power, torque, speed, and efficiency. The basic equations are shown below.

The power input to the motor is calculated by

$$VI = \left[2e_{ph} + 2IR_{ph} + 2V_{dd}\right]I \tag{11}$$

where,

e_{ph} = back emf generated per phase in the armature winding.

I = Armature current

R_{ph} = Resistance per phase of the armature winding

V_{dd} = Voltage drops in the device.

Back emf generated per phase in the armature winding

$$e_{ph} = 2B_g rlT_{ph}\omega_m \tag{12}$$

B_g = Flux density induction in the air gap

r = radius of the air gap

l = Length of the armature

T_{ph} = Turns per phase

ω_m = Angular Velocity.

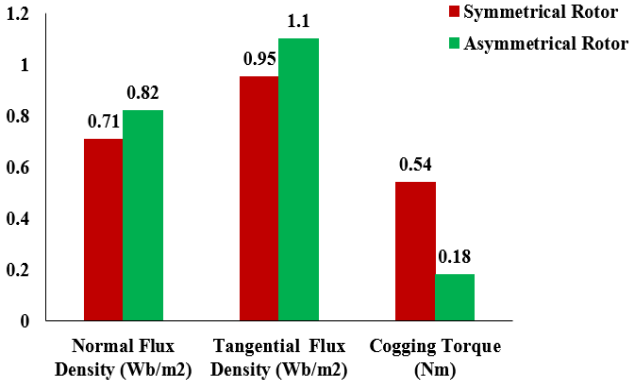

FIGURE 22. Comparison of Flux densities and Cogging Torque of symmetrical and asymmetrical rotor PMs.

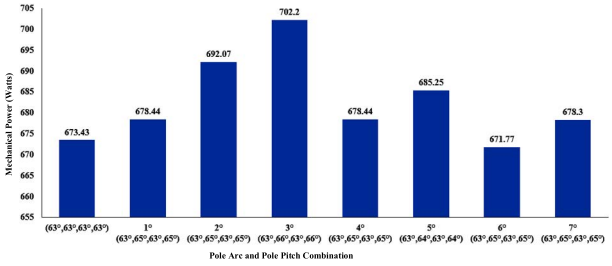

FIGURE 23. Comparison of mechanical power of BLDC motor with asymmetric rotor PMs.

The output power can be calculated as

$$\begin{aligned} P_m &= 2e_{ph}I \\ &= 4B_g r l T_{ph} \omega_m I \end{aligned} \tag{13}$$

Torque Developed in the motor

$$T = \frac{P_m}{\omega_m} = 4B_g r l T_{ph} I \tag{14}$$

The performance analysis was explained in detail previous chapter. Figure 23 shows the comparison of mechanical power of BLDC motor. The base model has the power 673.43 watts. The combination of 3° shift (A-B (87°), B-C (93°), C-D (87°), D-A (93°)) and pole arc (A-63°, B-66°, C-63°, D-66°) has 702.20 watts.

Figure 24 shows the comparison between mechanical torque of symmetrical and asymmetrical rotor structures and the conventional motor has mechanical torque of 1.29 Nm. Compared with the symmetrical structure all the asymmetrical structure has better mechanical torque. And the combination of 3° shift (A-B (87°), B-C (93°), C-D (87°), D-A (93°)) and pole arc (A-63°, B-66°, C-63°, D-66°) has attained the torque of 1.34 Nm.

Figure 25 shows the comparison of efficiency between the symmetrical and asymmetrical rotor structures where the conventional motor has efficiency 90.27%. Compared with symmetrical structure all the asymmetrical structures have better mechanical torque. And the combination of 3° shift (A-B (87°), B-C (93°), C-D (87°), D-A (93°)) and pole arc (A-63°, B-66°, C-63°, D-66°) has attained efficiency of 94.13%.

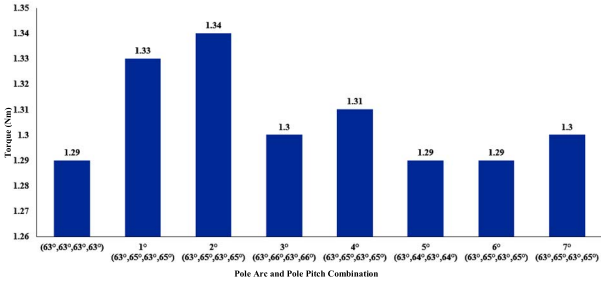

FIGURE 24. Comparison of torque of BLDC Motor with asymmetric rotor PMs.

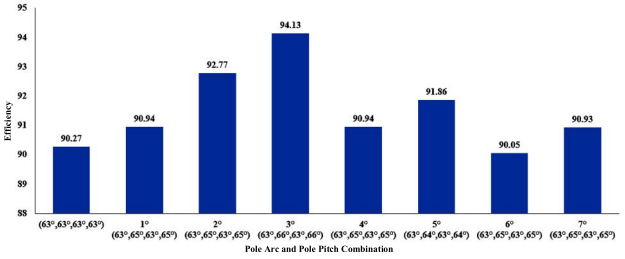

FIGURE 25. Comparison of efficiency of BLDC Motor with asymmetric rotor PMs.

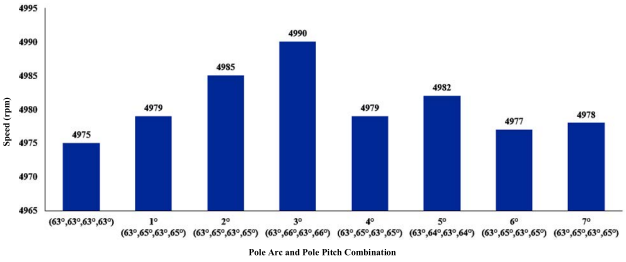

FIGURE 26. Comparison of speed of BLDC Motor with asymmetric rotor PMs.

Figure 26 shows the speed comparison of symmetrical and asymmetrical rotor structures where the conventional motor has speed 4975 rpm. Compared with symmetrical structure all the asymmetrical structures have better mechanical torque. And the combination of 3° shift (A-B (87°), B-C (93°), C-D (87°), D-A (93°)) and pole arc (A-63°, B-66°, C-63°, D-66°) has attained the speed of 4990 rpm.

Table 6 shows the comparison of speed, mechanical power, torque, and efficiency of conventional and various proposed designs of BLDC motor. From this analysis it is evident that the asymmetrical structure with pole pitch and pole arc combination (3° and 63°, 66°, 63°, 66°) has better performance compared with the base model and other proposed structures.

V. COMPARITIVE FEA ANALYSIS FOR COGGING TORQUE REDUCTION TECHNIQUES

The Simple Gradient Descent method helps to reduce the cogging torque by 2.72%, the Stator Claw Skewing technique reduces the cogging torque by 28%. The notches in stator minimizes the cogging torque up to 35.6% and closing the slot by sliding pre slot helps to reduce the cogging torque up to 47.8%. The hexagonal shapes of rotor magnets reduces 52% of the cogging torque and the reduction in magnet thickness

TABLE 6. Performance comparison after applying different pole pitch and pole arc combination.

	Mechanical power (watts)	Torque (Nm)	Speed (rpm)	Efficiency (%)
Base Model (63°,63°,63°,63°)	673.43	1.29	4975	90.27
1° (63°,65°,63°,65°)	678.44	1.30	4899	90.94
2° (63°,65°,63°,65°)	692.07	1.33	4900	92.77
3° (63°,66°,63°,66°)	702.20	1.34	4990	94.13
4° (63°,65°,63°,65°))	678.30	1.30	4890	90.93
5° (63°,64°,63°,64°)	685.25	1.31	4910	91.86
6° (63°,65°,63°,65°))	671.77	1.29	4977	90.05
7° (63°,65°,63°,65°))	678.44	1.30	4892	90.94

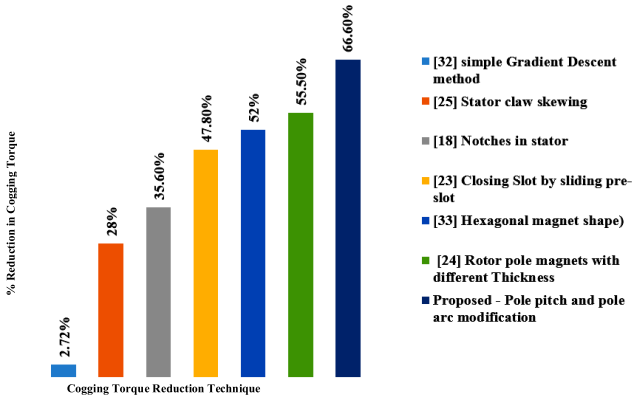

FIGURE 27. Comparison of cogging torque reduction techniques.

minimize the cogging torque up to 55.5%. While comparing with the existing techniques, the proposed technique based on pole pitch and pole arc change minimizes the cogging torque by 66.6%. Figure 27 shows the comparison of different cogging torque reduction techniques.

VI. CONCLUSION

This work offered a new cogging torque reduction method based on magnet shaping. The thickness of the permanent magnet is kept constant in this study. Pole pitch and pole arc are taken into account when making structural adjustments. For the best combination of pole pitch and pole arc, every feasible combination was tested. In this, combination of pole pitch (A-B (87°), B-C (93°), C-D (87°), D-A (93°)) and Pole Arc (A-63°, B-66°, C-63°, D-66°) get minimum cogging torque of 0.18 Nm. For analyzing the cogging torque reduction, an analytical expression is generated using VWM. The findings of the simulation and the analysis are compared. This asymmetrical shape results in a 66.6% reduction in cogging torque.

REFERENCES

[1] S.-M. Hwang, J.-B. Eom, G.-B. Hwang, W.-B. Jeong, and Y.-H. Jung, "Cogging torque and acoustic noise reduction in permanent magnet motors by teeth pairing," *IEEE Trans. Magn.*, vol. 36, no. 5, pp. 3144–3146, Sep. 2000.

[2] C. Breton, J. Bartolome, J. A. Benito, G. Tassinario, I. Flotats, C. W. Lu, and B. J. Chalmers, "Influence of machine symmetry on reduction of cogging torque in permanent-magnet brushless motors," *IEEE Trans. Magn.*, vol. 36, no. 5, pp. 3819–3823, Sep. 2000.

[3] N. Bianchi and S. Bolognani, "Design techniques for reducing the cogging torque in surface-mounted PM motors," *IEEE Trans. Ind. Appl.*, vol. 38, no. 5, pp. 1259–1265, May 2002.

[4] F. Caricchi, F. G. Capponi, F. Crescimbini, and L. Solero, "Experimental study on reducing cogging torque and no-load power loss in axial-flux permanent-magnet machines with slotted winding," *IEEE Trans. Ind. Appl.*, vol. 40, no. 4, pp. 1066–1075, Jul. 2004.

[5] T. Yoon, "Magnetically induced vibration in a permanent-magnet brushless DC motor with symmetric pole-slot configuration," *IEEE Trans. Magn.*, vol. 41, no. 6, pp. 2173–2179, Jun. 2005.

[6] Y. Yang, X. Wang, C. Zhu, and C. Huang, "Study of magnet asymmetry for reduction of cogging torque in permanent magnet motors," in *Proc. 4th IEEE Conf. Ind. Electron. Appl. (ICIEA)*, May 2009, pp. 2325–2328.

[7] D. A. Gonzalez, J. A. Tapia, and A. L. Bettancourt, "Design consideration to reduce cogging torque in axial flux permanent-magnet machines," *IEEE Trans. Magn.*, vol. 43, no. 8, pp. 3435–3440, Aug. 2007.

[8] K. Y. Hwang, S.-B. Rhee, B.-Y. Yang, and B.-I. Kwon, "Rotor pole design in spoke-type brushless DC motor by response surface method," *IEEE Trans. Magn.*, vol. 43, no. 4, pp. 1833–1836, Apr. 2007.

[9] P. S. Shin, S. H. Woo, Y. Zhang, and C. S. Koh, "An application of Latin hypercube sampling strategy for cogging torque reduction of large-scale permanent magnet motor," *IEEE Trans. Magn.*, vol. 44, no. 11, pp. 4421–4424, Nov. 2008.

[10] D. Lin, S. L. Ho, and W. N. Fu, "Analytical prediction of cogging torque in surface-mounted permanent-magnet motors," *IEEE Trans. Magn.*, vol. 45, no. 9, pp. 3296–3302, Sep. 2009.

[11] M. A. N. Doss, R. Brindha, K. Mohanraj, S. S. Dash, and K. M. Kavya, "A novel method for cogging torque reduction in permanent magnet brushless DC motor using T-shaped bifurcation in stator teeth," *Prog. Electromagn. Res. M*, vol. 66, pp. 99–107, 2018.

[12] J. H. Choi, J. H. Kim, D. H. Kim, and Y. S. Baek, "Design and parametric analysis of axial flux PM motors with minimized cogging torque," *IEEE Trans. Magn.*, vol. 45, no. 6, pp. 2855–2858, Jun. 2009.

[13] M. Fazil and K. R. Rajagopal, "A novel air-gap profile of single-phase permanent-magnet brushless DC motor for starting torque improvement and cogging torque reduction," *IEEE Trans. Magn.*, vol. 46, no. 11, pp. 3928–3932, Nov. 2010.

[14] M. Aydin and M. Gulec, "Reduction of cogging torque in double-rotor axial-flux permanent-magnet disk motors: A review of cost-effective magnet-skewing techniques with experimental verification," *IEEE Trans. Ind. Electron.*, vol. 61, no. 9, pp. 5025–5034, Sep. 2014.

[15] M. M. Rahman, K. T. Kim, and J. Hur, "Design and optimization of neodymium-free SPOKE-type motor with segmented wing-shaped PM," *IEEE Trans. Magn.*, vol. 50, no. 2, pp. 865–868, Feb. 2014.

[16] M. A. Noyal Doss, S. Vijayakumar, A. J. Mohideen, K. S. Kannan, N. D. B. Sairam, and K. Karthik, "Reduction in cogging torque and flux per pole in BLDC motor by adapting U-clamped magnetic poles," *Int. J. Power Electron. Drive Syst. (IJPEDS)*, vol. 8, no. 1, p. 297, Mar. 2017.

[17] M. A. N. Doss, K. Mohanraj, V. Kalyanasundaram, and K. Karthik, "Reduction of cogging torque by adapting bifurcated stator slots and minimization of harmonics and torque ripple in brushless DC motor," *Int. J. Power Electron. Drive Syst. (IJPEDS)*, vol. 7, no. 3, pp. 779–786, Sep. 2016.

[18] Y.-U. Park, J.-H. Cho, and D.-K. Kim, "Cogging torque reduction of single-phase brushless DC motor with a tapered air-gap using optimizing notch size and position," *IEEE Trans. Ind. Appl.*, vol. 51, no. 6, pp. 4455–4463, Nov./Dec. 2015.

[19] C.-M. Lee, H.-S. Seol, J.-Y. Lee, S.-H. Lee, and D.-W. Kang, "Optimization of vibration and noise characteristics of skewed permanent brushless direct current motor," *IEEE Trans. Magn.*, vol. 53, no. 11, pp. 1–5, Nov. 2017.

[20] M. Arun Noyal Doss, V. Ganapathy, V. Marthandan, and D. Mahesh, "Modeling and simulation of BLDC motor for minimizing the cogging torque, harmonics and torque ripples," *Int. Rev. Model. Simul.*, vol. 6, no. 5, pp. 1–6, Oct. 2013.

[21] M.-H. Hwang, H.-S. Lee, and H.-R. Cha, "Analysis of torque ripple and cogging torque reduction in electric vehicle traction platform applying rotor notched design," *Energies*, vol. 11, no. 11, p. 3053, Nov. 2018.
[22] T. A. Anuja and M. A. N. Doss, "Reduction of cogging torque in surface mounted permanent magnet brushless DC motor by adapting rotor magnetic displacement," *Energies*, vol. 14, no. 10, p. 2861, May 2021.
[23] M. García-Gracia, Á. J. Romero, J. H. Ciudad, and S. M. Arroyo, "Cogging torque reduction based on a new pre-slot technique for a small wind generator," *Energies*, vol. 11, no. 11, p. 3219, 2018.
[24] T. A. Anuja and M. Doss, "Asymmetrical magnets in rotor structure of a permanent magnet brushless DC motor for cogging torque minimization," *J. Elect. Eng. Technol.*, vol. 17, pp. 1271–1279, Jan. 2022.
[25] S. Leitner, H. Gruebler, and A. Muetze, "Cogging torque minimization and performance of the sub-fractional HP BLDC claw-pole motor," *IEEE Trans. Ind. Appl.*, vol. 55, no. 5, pp. 4653–4664, Sep. 2019.
[26] Z. Goryca, S. Różowicz, A. Różowicz, A. Pakosz, M. Leśko, and H. Wachta, "Impact of selected methods of cogging torque reduction in multipolar permanent-magnet machines," *Energies*, vol. 13, no. 22, p. 6108, Nov. 2020, doi: 10.3390/en13226108.
[27] K.-J. Han, H.-S. Cho, D.-H. Cho, and H.-K. Jung, "Optimal core shape design for cogging torque reduction of brushless DC motor using genetic algorithm," *IEEE Trans. Magn.*, vol. 36, no. 4, pp. 1927–1931, Jul. 2000.
[28] M. Markovic, M. Jufer, and Y. Perriard, "Reducing the cogging torque in brushless DC motors by using conformal mappings," *IEEE Trans. Magn.*, vol. 40, no. 2, pp. 451–455, Mar. 2004.
[29] S.-K. Lee, G.-H. Kang, J. Hur, and B.-W. Kim, "Stator and rotor shape designs of interior permanent magnet type brushless DC motor for reducing torque fluctuation," *IEEE Trans. Magn.*, vol. 48, no. 11, pp. 4662–4665, Nov. 2012.
[30] K. J. Kang, G. H. Jang, and S. J. Sung, "Frequency characteristics of BEMF, cogging torque and UMF in a HDD spindle motor due to unevenly magnetized PM," *IEEE Trans. Magn.*, vol. 49, no. 6, pp. 2578–2581, Jun. 2013.
[31] H.-S. Kim, Y.-M. You, and B.-I. Kwon, "Rotor shape optimization of interior permanent magnet BLDC motor according to magnetization direction," *IEEE Trans. Magn.*, vol. 49, no. 5, pp. 2193–2196, May 2013.
[32] D. Wang, X. Wang, M.-K. Kim, and S.-Y. Jung, "Integrated optimization of two design techniques for cogging torque reduction combined with analytical method by a simple gradient descent method," *IEEE Trans. Magn.*, vol. 48, no. 8, pp. 2265–2276, Aug. 2012.
[33] H. Usman, J. Ikram, K. S. Alimgeer, M. Yousuf, S. S. H. Bukhari, and J.-S. Ro, "Analysis and optimization of axial flux permanent magnet machine for cogging torque reduction," *Mathematics*, vol. 9, no. 15, p. 1738, Jul. 2021.
[34] Y. Yang, X. Wang, R. Zhang, T. Ding, and R. Tang, "The optimization of pole arc coefficient to reduce cogging torque in surface-mounted permanent magnet motors," *IEEE Trans. Magn.*, vol. 42, no. 4, pp. 1135–1138, Apr. 2006.

T. A. ANUJA received the A.M.I.E. degree in electrical engineering from the Institution of Engineers, India, in 2007, and the M.E. degree in power system from Anna University, in 2009. She is currently pursuing the Ph.D. degree in electrical engineering from SRM University. Her research interests include power systems and special machines.

ARUN NOYAL DOSS M. received the B.E. degree in electrical engineering from Madras University, in 2004, the M.E. degree in power electronics and drives from Anna University, in 2006, and the Ph.D. degree in electrical engineering from SRM University, in 2014. He is currently working as an Associate Professor at SRM University. His research interests include power electronics, modeling of electrical machines, and special machines.

R. SENTHILKUMAR was born in Chinnamanur, Tamil Nadu, India, in May 1976. He received the B.E. degree in electrical and electronics engineering from the Thiagarajar College of Engineering, Madurai Kamaraj University, Madurai, India, the M.Tech. degree in instrumentation and control engineering from Bharat University, Chennai, Tamil Nadu, and the Ph.D. degree from the SRM Institute of Science and Technology, Chennai, in 2020. He is currently working as an Assistant Professor of electrical and electronics engineering at the Department of EEE, SRM Institute of Science and Technology. He has published 19 research papers in international journals. His research interests include power electronics, digital signal processing, microcontroller, soft computing, VLSI design, image processing, neural networks, and fuzzy logic.

RAJESH K. S. (Member, IEEE) was born in Trivandrum, Kerala, India, in 1986. He received the B.Tech. degree in electrical and electronics engineering from the University of Kerala, India, in 2008, the M.Tech. degree in power system from the College of Engineering, Trivandrum, in 2012, the Ph.D. degree in power system from SRM University, Chennai, India, in 2019, and the M.B.A. degree specialization in power management and advanced diploma in industrial safety (HSE) from the University of Petroleum and Energy Studies, Dehradun, India, in 2020 and 2021, respectively. In 2020, he joined the Department of Power Management, School of Business, University of Petroleum and Energy Studies, as an Assistant Professor. His current research interests include power system control, electrical machines, power markets, power system regulation, and renewable energy policy. He is a Life Time Member of Indian Society for Technical Education (ISTE).

R. BRINDHA received the B.E. degree from the Easwari Engineering College, Madras University, in 2002, the M.Tech. degree in power electronics and drives from SRM University, and the Ph.D. degree in ped from SRM University, in 2017. Her research interests include renewable energy, power electronics, and research on controller design and drive.